

B012

Automatic Migration Velocity Analysis Using Reverse Time Migration

W.W. Weibull* (Norwegian University of Science and Technology) & B. Arntsen (Norwegian University of Science and Technology)

SUMMARY

The objective of this paper is to describe an automatic velocity analysis method based on Reverse Time Migration and Differential Semblance Optimization. The velocity analysis is based on the solution of a nonlinear least squares problem aiming at the focusing of offset domain common image point gathers constructed by Reverse Time Migration. Because the method is based on the solution of the two-way wave equation, it can deal with strong and sharp velocity contrasts both in a stable and accurate manner. It is therefore expected that this method will help improve seismic imaging over complex geological settings. We illustrate the method with a simple synthetic 2D seismic example.

Introduction

Reverse Time Migration (RTM) (Baysal et al., 1983) has, during recent years, become an important tool for imaging subsurface structures characterized by complex velocity fields. The image quality is strongly dependent on the properties of the employed velocity model, which routinely is built through a combination of ray-based tomography and a range of trial-and-error procedures. Tarantola (1984) introduced waveform inversion, which aims at automatic estimation of velocity models by minimizing the error between simulated synthetic data and observed data.

An alternative to Tarantola (1984)'s method was introduced by Biondi and Sava (1999) which suggested to perform velocity analysis by minimizing errors in the image space by using one-way migration schemes. A problem with both Biondi and Sava (1999) and Tarantola (1984)'s approaches is the reliance on the validity of the born approximation, which can limit the utility of the methods (Weibull and Arntsen, 2010) unless additional measures are taken (Sava and Biondi, 2004).

Shen et al. (2003) and Shen and Symes (2008) suggested to use an error function based on differential semblance (Symes and Carazzone, 1991) which reduces, but do not completely overcome, the problems caused by the Born approximation. Shen and Symes (2008)'s method relies on a one-way shot-migration algorithm, which in principle can be extended to a two-way reverse-time migration algorithm, as suggested by Gao and Symes (2009). However, a straightforward implementation of migration velocity analysis based on two-way reverse time migration and differential semblance, leads to an algorithm with non-optimal convergence properties.

In this paper we show that by modifying the imaging condition with a differential operator, a stable RTM differential semblance algorithm with better convergence properties is obtained, as illustrated with simple synthetic examples.

Theory and Method

The objective of Differential Semblance Optimization (DSO) is to estimate an unknown velocity field by focusing the energy of offset domain Common Image Points (CIPs) at zero offset, which is equivalent to flattening the angle domain CIPs (Shen and Symes, 2008).

We start by defining our differential semblance misfit function:

$$DS = \frac{1}{2} \|h\Delta_z R\|^2 = \frac{1}{2} \int dx \int dh \int dz h^2 (\Delta_z R(x, h, z))^2, \quad (1)$$

where, h is the subsurface half-offset, x, z are spatial coordinates, R is the migrated image volume, and Δ_z is a first order derivative filter operator, such that:

$$\Delta_z R(x, h, z) = R(x, h, z) - R(x, h, z - \Delta z), \quad (2)$$

with $\Delta_z R(x, h, 0) = 0$ and Δz is the vertical depth interval.

In reverse time migration, R is constructed according to the multi-offset crosscorrelation *imaging condition* (Rickett and Sava, 2002):

$$R(x, h, z) = \sum_s \sum_t U(x + h, z, t, s) D(x - h, z, t, s). \quad (3)$$

Where s represents the source index, t is the time index, D is the forward modeled source wavefield, and U is the reflected wave field, reverse time extrapolated from the receivers.

The velocity analysis consists of minimizing equation 1 with respect to the P-wave velocity $c(x, z)$. One of the advocated properties of equation 1 is its convexity, which allows optimization by gradient based

methods (Symes, 2008). Thus, all that needs to be computed is the the gradient of the misfit function with respect to velocity.

The derivative of equation 1 with respect to velocity $c(x, z)$ can be efficiently computed through the adjoint state method (Chavent, 2009). The gradient is then given by:

$$\nabla_c DS(x, z) = - \sum_s \sum_t \frac{2}{c^3(x, z)} \frac{\partial^2 D}{\partial t^2}(x, z, t, s) D'(x, z, t, s), \quad (4)$$

$$- \sum_s \sum_t \frac{2}{c^3(x, z)} \frac{\partial^2 U}{\partial t^2}(x, z, t, s) U'(x, z, t, s), \quad (5)$$

where $U'(x, z, t, s)$ and $D'(x, z, t, s)$ are adjoint states associated with the constraints that the direct states U and D must satisfy the isotropic constant density acoustic wave equation.

By introducing the Green's function:

$$\left(\frac{1}{c^2(x, z)} \frac{\partial^2}{\partial t^2} + \nabla^2 \right) g(x, z, t; x', z', t') = \delta(x - x') \delta(z - z') \delta(t - t'), \quad (6)$$

D' and U' are then found to be the solutions of two simulations:

$$D'(x, z, t, s) = \int dx' \int dz' g(x, z, 0; x', z', t) * \left(\int dh h^2 \Delta_z^2 R(x' + h, h, z') U(x' + 2h, z', t, s) \right), \quad (7)$$

$$U'(x, z, t, s) = \int dx' \int dz' g(x, z, t; x', z', 0) * \left(\int dh h^2 \Delta_z^2 R(x' - h, h, z') D(x' - 2h, z', t, s) \right), \quad (8)$$

where $*$ denotes time convolution, and Δ_z^2 is a second order centered finite difference operator such that:

$$\Delta_z^2 R = R(x, h, z + \Delta z) - 2R(x, h, z) + R(x, h, z - \Delta z), \quad (9)$$

with $\Delta_z^2 R(x, h, 0) = \Delta_z^2 R(x, h, NZ) = 0$.

Equation 7 is to be solved in reverse time, while equation 8 is to be solved in forward time.

A step by step procedure to compute the gradient follows:

1. Construct R , and at the same time store the direct states U and D for each shot.
2. Perform the two simulations for each shot, according to equations 7 and 8, to compute the adjoint states D' and U' , and at each time step use equations 4 and 5 to build, respectively, the source and receiver parts of the gradient.
3. Stack the source and receiver parts of the gradient over all shots to obtain the full gradient.

Example

We illustrate the method with a synthetic 2D seismic example. The example is interesting because it shows the potential of the method to improve an image even when the initial model is very far from the true model, but at the same time it shows some of the associated pitfalls.

The true velocity model is shown in figure 1A. It consists of a layered model 3.6km long and 900 m deep, with a small structure in the middle. The top of the structure coincides with the center of a low velocity lens, where velocities are reduced by up to 500 m/s. The data consist of 181 shots simulated at the top of the model, with 20 m spacing. The source is a Ricker wavelet with dominant frequency of 25 Hz. The

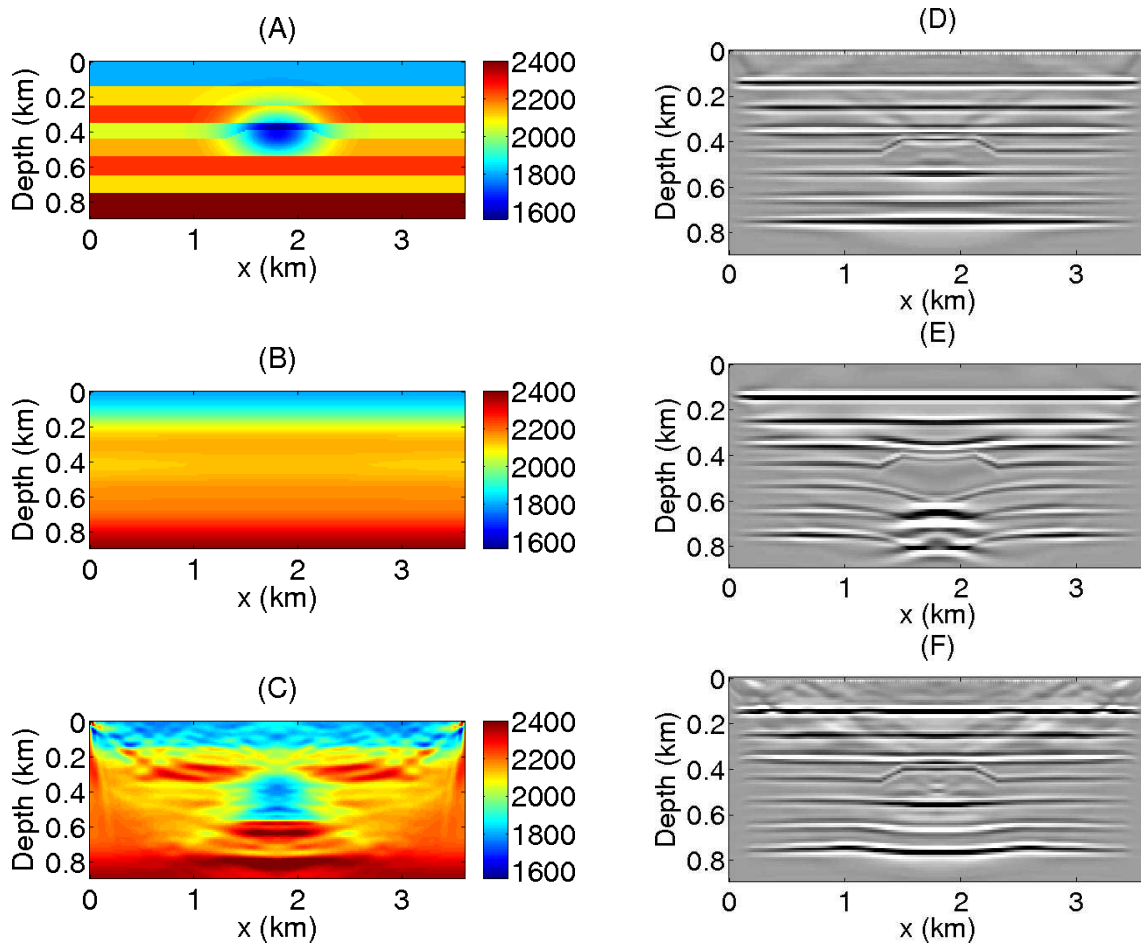


Figure 1 (A)-True velocity model; (B)-Initial velocity model; (C)- Updated velocity model after 50 iterations; (D)- RTM Image produced using true velocity model; (E)- RTM image produced using initial velocity model; (F)-RTM Image produced using updated velocity model after 50 iterations.

receiver line consist of 361 receivers fixed at the top of the model with 10 meter spacing between the receivers and recording length of 1.75 seconds. The data is simulated with absorbing boundaries at all sides. Preprocessing consists of subtracting the direct wave, FK filtering to remove highly dipping plane waves and refractions.

The initial model for the DSO consists of a smoothed version of the layered model, where the structure and the low velocity lens are ignored (fig.1B).

Equation 1 is optimized using a limited memory quasi-Newton method (Nocedal and Wright, 2000). No regularization is used, but the gradient is low pass filtered with zero gain at the nyquist wavenumber. This is to remove effects of numerical dispersion. The velocity model after 50 updates is shown in figure 1C. We can see that it compares favourably with the true velocity model. Some considerations have to be taken though: The velocity seems to be updated mainly in the region where there is enough angle coverage, which is a consequence of our simulated acquisition geometry. Another consideration is with respect to the resolution attainable by velocity analysis by DSO, which is clearly limited by the bandwidth of the seismic data. But to what extent it is so, would be the subject of more research.

Figures 1D, 1E, and 1F show a comparison of the RTM images computed using the true, initial and updated velocities. While Figure 2 shows similar comparison of the CIPs at $x = 1.8km$. The images clearly show that the updated velocity model substantially improves the image. The CIPs show that

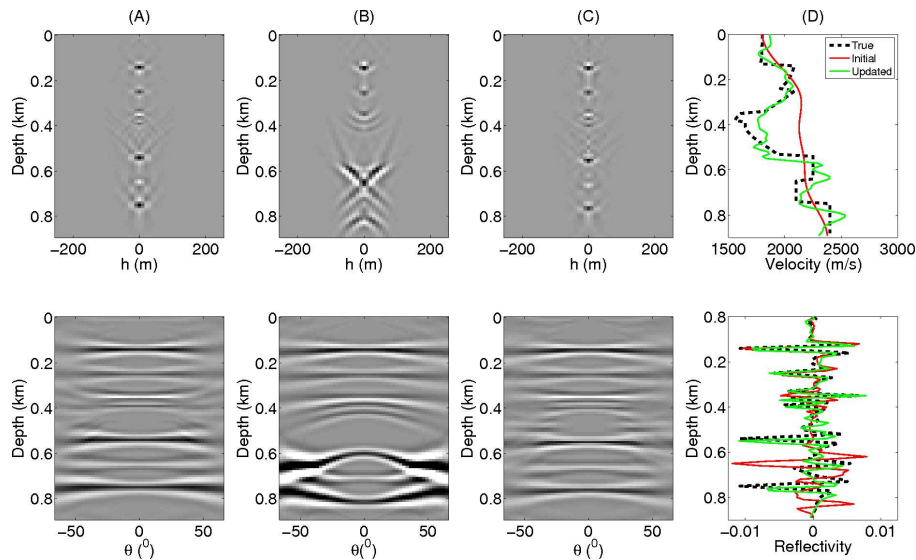


Figure 2 (A)-Offset domain (*top*) and angle domain (*bottom*) CIPs at $x = 1.8$ km, computed using the true velocity model; (B)-Same as (A) but using initial velocity model; (C)- Same as (A) but using the updated velocity model after 50 iterations; D- Velocity profiles (*top*) and reflectivity profiles (*bottom*) at $x = 1.8$ km.

optimization improves focusing of the offset domain CIPs, and consequently the flattening of corresponding angle domain CIPs. Figure 2D also shows vertical profiles of the velocity (top) and zero offset reflectivity (bottom), for spatial position $x = 1.8$ km.

Conclusions

Introducing a vertical differentiation operator in the differential semblance misfit function allows for automatic velocity analysis using RTM. This should in principle allow for more accurate and stable velocity analysis in areas of strong velocity contrasts. Our simple example illustrates the capability of RTM based DSO to improve the image even when the initial velocity model is far from the true model.

Acknowledgements

The authors acknowledge the financial support of Statoil and the sponsors of the ROSE consortium.

References

- Baysal, E., Kosloff, D.D. and Sherwood, J.W.C. [1983] Reverse time migration. *Geophysics*, **48**(11), 1514–1524.
- Biondi, B. and Sava, P. [1999] Wave-equation migration velocity analysis. *SEG, Expanded Abstracts*, **18**(1), 1723–1726.
- Chavent, G. [2009] *Nonlinear Least Squares for Inverse Problems. Theoretical Foundations and Step by Step Guide for Applications*. Springer.
- Gao, F. and Symes, W. [2009] Differential semblance velocity analysis by reverse time migration: Image gathers and theory. *SEG, Expanded Abstracts*, **28**(1), 2317–2321.
- Nocedal, J. and Wright, S.J. [2000] *Numerical Optimization*. Springer.
- Rickett, J.E. and Sava, P.C. [2002] Offset and angle-domain common image-point gathers for shot-profile migration. *Geophysics*, **67**(3), 883–889.
- Sava, P. and Biondi, B. [2004] Wave-equation migration velocity analysis. I. theory. *Geophysical Prospecting*, **52**(6), 593–606.
- Shen, P. and Symes, W.W. [2008] Automatic velocity analysis via shot profile migration. *Geophysics*, **73**(5), 49–59.
- Shen, P., Symes, W.W. and Stolk, C.C. [2003] Differential semblance velocity analysis by wave-equation migration. *SEG, Expanded Abstracts*, **22**(1), 2132–2135.
- Symes, W.W. [2008] Migration velocity analysis and waveform inversion. *Geophysical Prospecting*, **56**(6), 765–790.
- Tarantola, A. [1984] Inversion of seismic reflection data in the acoustic approximation. *Geophysics*, **49**(8), 1259–1266.
- Weibull, W. and Arntsen, B. [2010] Implications of the born approximation for WEMVA - a systematic approach. *SEG, Expanded Abstracts*, **29**(1), 4405–4409.